# BIODEGRADABLE PLA COATINGS WITH IMPROVED PROPERTIES USING SCALABLE $TiO_2/SiO_2$ CORE-SHELL PIGMENTS FOR SUGARCANE BAGASSE PACKAGING PAPER

ABEER M. ADEL,[*] NIVIN M. AHMED,[**] AMAL H. ABDEL KADER,[*]
MONA T. AL-SHEMY[*] and MONA A. EL-SABOUR[*]

[*]*Cellulose and Paper Department, National Research Centre, 33 El-Bohouth Str.*
*(Former El-Tahrir Str.), P.O. 12622, Dokki, Giza, Egypt*
[**]*Polymers and Pigments Department, National Research Centre, 33 El-Bohouth Str.*
*(Former El-Tahrir Str.), P.O. 12622, Dokki, Giza, Egypt*
✉ *Corresponding author: A. M. Adel, abeermadel2003@yahoo.com, am.adel@nrc.sci.eg*

*Received* December 8, 2024

This study focuses on the development of coating films composed of biodegradable polylactic acid combined with the new $TiO_2/SiO_2$ core-shell pigment for enhancing the properties of paper sheets used in packaging, besides overcoming the limitations of its individual components. The study proceeded through investigating the impact of the different pigment concentrations on the structural, mechanical and barrier properties of the coated paper. Coated papers with biodegradable materials are essential for improving their different properties, such as density, surface gloss, smoothness, and moisture resistance. The core-shell pigment that was prepared in this study using a very simple chemical technique based on the co-precipitation of the $TiO_2/SiO_2$ components at specific temperature and pH can offer advanced properties by overcoming the deficiencies of both titanium and silicon dioxides individually through their combination in a new compound with improved properties, which can provide advanced packaging papers of low cost. Different concentrations (0.25%, 0.5%, 1%, and 2%) of core-shell $TiO_2/SiO_2$ were mixed with PLA, and the resulting formulations were used to coat the paper sheets. The corresponding physical and chemical properties were assessed using FTIR, TGA, TEM, SEM, and EDX. Furthermore, the mechanical strength and water vapor characteristics of the paper sheets treated with PLA-$TiO_2/SiO_2$ were assessed. The findings were satisfying, which can contribute to the progress of sustainable and functional packaging materials, as well as emphasizing the importance of core-shell pigments in improving the performance of such materials.

***Keywords***: core-shell, pigments, $TiO_2/SiO_2$, paper coating, polylactic acid (PLA)

## INTRODUCTION

Paper is a highly versatile material, with various favorable properties, *e.g.* biodegradability, renewability, recyclability, mechanical flexibility, and affordability. It is mainly made of cellulosic fibers derived from renewable natural bioresources, including wood and non-wood lignocellulosic biomass.[1,2] Agricultural residues represent an abundant source of lignocellulosic biomass, in Egypt alone, approximately 30-35 million tons of agricultural residues are produced annually. The burning process of these wastes, which is the most frequently used method of disposal, causes severe pollution of land and water, on both local and regional scales. Besides, during this process, the carbon, nitrogen, and sulfur from the biomass are completely burned, resulting in the emission of smoke, which reacts with gases present in the air, like methane, nitrogen oxide and ammonia, causing severe atmospheric pollution.[3] These gaseous emissions cause health risks and contribute indirectly to increased atmosphere pollution. Thus, reusing agricultural residues (*e.g.* bagasse) at an industrial level is preferable, and this study was carried out based on these considerations.

Paper is normally characterized by some drawbacks, such as high porous structure, poor grease resistance and water vapor permeability. These drawbacks negatively affect the quality of the paper employed in packaging. Coating materials applied to paper sheets via various approaches help overcome these limitations, research in this area has lately enhanced the suitability of paper for packaging applications.[4] Besides the protection of the paper surfaces from moisture, grease and water, the coating process is done to impart certain characteristics to the paper, including density, surface gloss, and smoothness.

The most widely used coating materials are thin laminated-plastic films or liquid polymeric coats (*e.g.*, polypropylene (PP), polyvinyl chloride (PVC), polyvinylidene chloride (PVdC), polyethylene (PE), polystyrene (PS) and polyethylene terephthalate (PET)), but these materials are not susceptible to biodegradability and therefore can cause several environmental issues because of the increase in the percentage of non-degradable packaging wastes.[5] This phenomenon has stimulated research interest in producing natural polymer-based biodegradable packaging systems. Bio-based polymers, originating from renewable sources, have recently garnered attention as environmentally friendly alternatives to traditional plastic packaging materials, owing to their capacity to diminish the environmental impact. Biopolymers, such as chitosan, cellulose[6,7] and alginate, have been recently developed as viable and biocompatible alternatives to the petroleum-based polymers.[8,9]

Biodegradable plastics, and among them polylactic acid (PLA), are considered as very promising materials in this area, due to their thermo-plasticity, biodegradability, biocompatibility, high strength, high modulus and good processability. PLA is a linear aliphatic thermoplastic polyester produced either by the poly-condensation of lactic acid or by the ring opening polymerization of lactide.[10, 11] Since PLA is a highly transparent and rigid plastic, with high mechanical properties, it was always used for the fabrication of various products, such as trays, cups, tubs, and films.[12,13] However, its brittleness and other properties, such as low thermal stability, medium gas barrier properties, low solvent resistance, high rigidity, low toughness and ductility of the pure polymer, are often disappointing properties that restrain the use of PLA in packaging applications.[14] To overcome such deficiencies, PLA can be blended with fillers, such as clay,[15] cellulose fibers,[16] microcrystalline cellulose[17] and metals[18] to improve its physical, mechanical and antimicrobial properties.[19]

Among metallic or metal oxide fillers, titanium and silicon dioxides are outstanding, since they possess several desired properties, such as availability, low cost, stability, high ultraviolet absorption capacity, and antimicrobial activity. These metal oxides are considered as potential candidates for reinforcing the polymer matrix to support their application in packaging. Silica ($SiO_2$) is one of the most common materials on the earth, it exists in pure form or with other metal oxides. Because of its stability and high heat resistance, silica particles have been investigated in various fields.

On the surface of $SiO_2$, there are several large hydrophilic hydroxyl groups, and combining these hydrophilic particles with hydrophobic PLA is considered as the key challenge in this present work.[20] $TiO_2$ is commonly used in paper products to increase opacity and brightness. Besides its conventional use to produce high value-added printing paper, its presence can aid numerous properties of the composite films, such as mechanical and gas barriers that are decisive properties for the application in packaging.[21] Core-shell particles are new structural tailored particles that contain more than one component in the same structure that are prepared using a very simple chemical technique at specific temperature and pH. Therefore, they can convey unique properties in functional materials for many fields of application. The right choice of the different components in these structured particles can lead to superior properties that can overcome the deficiencies of its individual components and can offer more value-added characteristics. Coating the paper surface with a film containing PLA/core-shell pigments can offer admirable assets to the paper, including weight, surface smoothness, opacity, gas permeability, and reduced ink absorbency.

Coating techniques of paper surfaces are numerous; these techniques include extrusion coating, dip coating, rod coating, spray coating, and knife coating. The dip coating method is considered the easiest and fastest method, since it only requires immersing the paper sheets into a solution; and after the coating material has been deposited on the surface, the substrate is left to completely dry.[22]

PLA-$TiO_2$/$SiO_2$ composite films were prepared by solution casting and electrospinning methods, respectively. Hybrid materials were created via the solution casting through dispersing the nanoparticles directly into a polymer matrix. Electrospinning is a promising method for the surface coating process for *in situ* generated nanoparticles or in the bulk of a polymer matrix.

The differences between the prepared nanocomposite membranes by the two methods were determined considering the application of the materials in antimicrobial packaging.[23,24]

The main objective of this study has been to assess the different properties of paper sheets coated with films comprising PLA-$TiO_2/SiO_2$ core-shell pigments. The core-shell pigments developed in this study comprise different thicknesses of the shell containing titanium dioxide, which means that different loadings of the titanium dioxide are situated on the surface. Studying the effect of the pigments with different titanium dioxide shells is the main goal in this study, followed by the determination of different loadings of the core-shell pigment as a whole within the range of 0.25-2% in combination with PLA, to clarify their optimum concentration to be used with PLA for the finest properties of the coated paper sheets. These different assessments were done by testing the structural, mechanical and barrier properties of the covered paper sheets.

## EXPERIMENTAL

### Materials

Silica fume ($SiO_2$) is a by-product, representing a gray powder with the specific gravity of 2.22, particle size of 100-200 µm and pH of 6.5 obtained from the ferrosilicon and other metal alloy factories in Aswan, Egypt.

Quena Company of the pulp and paper sector (Cairo, Egypt) kindly provided the bagasse fibers. Based on TAPPI standard processes, the chemical composition of the raw bagasse material was as follows: 41.50% α-cellulose (T 203 cm-99), 27.20% hemicelluloses (T-223 cm-84), 20.40% lignin (T-222 om-88), and 1.80% ash (T-211 om-02). The data is represented as the mean value for each set of measurements, which were all performed in triplicate.

The raw bagasse material was treated with 15% NaOH, 5% $Na_2S$ (as $N_2O$), and 0.05% anthraquinone (AQ)-based on oven-dry raw material at 160 °C for two hours and 1:6 liquor ratios using a hydrothermal autoclave reactor. After that, the pulp was bleached via the typical three-stage method: first, the chlorine dioxide ($D_0$-Stage) by adding 10% $ClO_2$ based on oven-dry pulp with 10% $H_2SO_4$ for adjusting pH at 60-65 °C for an hour; second, the oxygen stage (EO-Stage) by adding 10% ($H_2O_2 + O_2$) in the presence of 10% $H_2SO_4$ at 60-65 °C for one and a half hours; and third, the chlorine dioxide stage ($D_1$-Stage) 5% $ClO_2$ based on oven-dry pulp with 10% $H_2SO_4$ at 60-65 °C for a duration of four hours. After several washings, the bleached kraft bagasse pulp was exposed to refinery disks at 40-45 °SR using Tappi's standard techniques to analyze the bleached kraft bagasse pulp: 73.70% α-cellulose (T203 om-83), 24.40% pentosane (T223 om-84), and 1.18% lignin (T 222 om-88).

PLA (6202D fiber grade) was acquired from Nature Works, USA; its density was 1.24 g/cc, with melt flow index of 15-30 g/10 min and average molecular weight of 44350 $g{\cdot}mol^{-1}$. It was dried at 80 °C for 4 hours in a vacuum oven before processing. All other used chemicals were of analytical grade and purchased from Sigma-Aldrich (St. Louis, MO, USA).

### Preparation of $TiO_2/SiO_2$ core-shell pigment

The preparation method in this study consisted in the co-precipitation of titanium dioxide on the surface of silica fume. Consequently, titanium tetrachloride was exploited as the precursor for titanium dioxide, and hence three different concentrations (1, 2 and 3 mL) were added to 100 mL of hydrochloric acid. Then, the silica particles were immersed in these solutions, allowing complete coverage. To adjust the pH of the prepared pigment to be neutral and facilitate the precipitation, ammonia solution was added dropwise. The reaction resulted in a paste, which was subsequently filtered using a Buchner system and extensively washed. Finally, the paste was subjected to calcination at temperatures ranging between 600-750 °C.[1,6] Lastly, three core-shell pigments were obtained with different shell ($TiO_2$) concentrations, and they were denoted as $TiO_2/SiO_2$ (1), $TiO_2/SiO_2$ (2) and $TiO_2/SiO_2$ (3).

### Preparation of PLA-($TiO_2/SiO_2$) nanocomposite

A PLA solution (10 wt%) was prepared in chloroform by stirring the pellets at 60 °C for 2 h until totally dissolved. Then, after complete dissolution, the different core-shell pigments: $TiO_2/SiO_2$ (1), $TiO_2/SiO_2$ (2) and $TiO_2/SiO_2$ (3), were added in different concentrations (0.25%, 0.50%, 1% and 2%) and stirred using a homogenizer at room temperature for 20 min to reach homogeneous mixing of the metal oxides ($TiO_2/SiO_2$) by effective impregnation in the PLA solution. The last step was using ultrasonication to remove suspended gas bubbles from the liquid and reduce dissolved gas below the natural equilibrium level.

### Handsheet preparation

Bleached kraft bagasse pulp was beaten in a Valley beater till 30 °SR, and paper sheets were prepared according to the Swedish Standard Method (SCAN-CM 64:00). Handsheets of basis weight of 68 $g/m^2$ were formed. Five paper sheets for each sample series were coated with different concentrations of PLA-($TiO_2/SiO_2$) suspension (0.25%, 0.50%, 1%, and 2%) using the dipping method. The procedure of coating proceeded as follows: first, the paper sheets were immersed for 60 seconds in PLA-($TiO_2/SiO_2$) suspensions; then, after each immersion step, the paper was removed from the suspension after the film composite has been deposited on the surface; the coated samples were dried and finally left in an oven at 65 °C for 2 h. All paper samples were conditioned before measurements at 23 °C and relative humidity (RH) of 50% for 24 h before analysis. The process is illustrated in Figure 1.

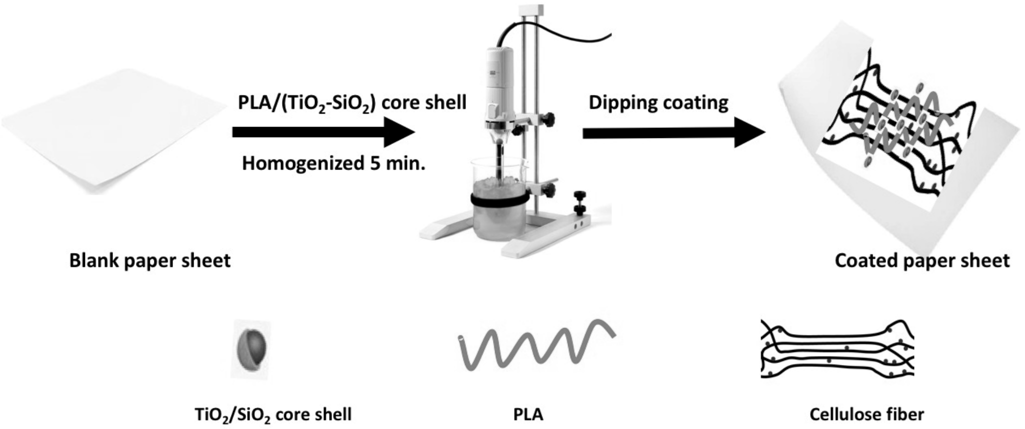

Figure 1: Graphical representation for paper sheets coated with PLA-$TiO_2$/$SiO_2$ core shell system

**Instrumental analysis**

**X-ray diffraction (XRD)**: X-ray powder diffraction (XRD) patterns were obtained at room temperature using a Philips diffractometer (Model PW 1390), Japan, employing Ni-filtered Cu Kα radiation ($\lambda = 1.5404$ Å). The diffraction angle (2θ) was scanned at a rate of 2 °/min.

**X-ray fluorescence (XRF)**: the different concentrations of each oxide element in the prepared pigments were determined using an Axios Sequential WD-XRF Spectrometer, PANalytical 2005, USA.

**TEM analysis**: a JEOL JEM 2100 (Japan), with a micro-analyzer electron probe, was used to determine the different particle shapes and sizes of the prepared pigments.

**SEM/EDAX analysis**: Energy-dispersive X-ray (EDAX) analysis and scanning electron microscopy (SEM) (JEOL JX 2840) with a micro-analyzer electron probe (Japan) were used in this work to study the surface morphology of the pigments, as well as the surfaces of the reference and coated papers. The test samples were mounted on specimen stubs and examined by SEM at an accelerating voltage of 10 kV with a tilt angle of 45°. The surface pore area of the prepared paper sheets was estimated using Image J, an open-source image analysis program.

**Attenuated total reflectance Fourier transform infrared spectroscopy**: ATR-FTIR spectra of papers treated with PLA-$TiO_2$/$SiO_2$ composites were recorded on a Shimadzu IR Prestige-21, equipped with a single reflection ATR-8200HA accessory, mounting a Zn-Se crystal tip. The spectra are collected as the average of at least 200 scans in the frequency range of 4000-500 $cm^{-1}$, at a resolution of 4 $cm^{-1}$.

**Thermal analysis**: an AC7/DX TGA7 (Perkin-Elmer) was used to record simultaneously the TG and DTG curves for coated paper sheets. The experiments were carried out in dynamic nitrogen atmosphere (20 mL/min), with a heating rate of 10 °C/min in the temperature range within 20-600 °C using platinum crucibles. The kinetic parameters, such as thermodynamic energy of activation ($E_a$), for the main combustion step were evaluated graphically by using the method of Coats-Redfern:[25]

$$\ln [Y/T^2] = \ln [AR/gE_a] - E_a/RT \quad (1)$$

where $Y = \ln (W_f / W_f - W)$, $W_f$ and W are the final and actual weight of the samples, respectively, up to temperature T; R is the gas constant, A is the pre-exponential factor and g is the heating rate.

**Mechanical strength properties**

Mechanical strength properties, *e.g.* tensile, burst, and tear indices, of the paper sheets were determined according to TAPPI standards. Average and standard deviation (SD) for the measurements was calculated based on five replicates for each sample. Tensile strength testing was measured according to TAPPI (T494-06) standard method using a universal testing machine (LR10K; Lloyd Instruments, Fareham, UK), with a 100-N load cell at a constant crosshead speed of 2.5 cm/min. Strips of 10 cm long and 15 mm wide were used in the test, and the span was set at 10 cm. Tear resistance was carried out with an Elmendorf type tear tester (Thiwing-Albert Instrument Co, Philadelphia, PA) using TAPPI (T414-04) standard method. Burst strength was measured according to TAPPI standard test method T403 om-10 using Mullen Testers (Chicopee, MA, USA). The coated layer amount of PLA-($TiO_2$/$SiO_2$) on paper sheets and the bulk density were calculated using the following equations:

$$\text{Coated Layer}\left(\frac{g}{m^2}\right) = \frac{(W_2 - W_1)\ (g)}{\text{Area of coating}\ (m^2)} \quad (2)$$

$$\text{Bulk denisty}\left(\frac{Kg}{m^3}\right) = \frac{\text{Basis wieght}\left(\frac{Kg}{m^2}\right)}{\text{Thikness}\ (m)} \quad (3)$$

**Barrier properties of paper sheets**

**Water vapor permeability (WVP)** was assessed according to ASTME96/E96M-10. Paper sheets under the study were conditioned at 50% RH and 25 °C for 24 h before being applied to seal cover aluminum cups holding 5 g of anhydrous calcium chloride. The bare side of coated paper is the one that faces the dehydrated region; the WVP was estimated employing Equation (4):

$$\mathrm{WVP} = g \times h / t \times A \times \Delta P \qquad (4)$$

where (g/t) is the slope of the plot between the obtained weight (g) and time (t), h is the average thickness of the papers, A is the infiltration area, and ΔP is the partial water vapor pressure variance (≈2385 Pa) between the saturated sodium chloride solution (75% RH) outside and the air inside the cup (0% RH). The final WVP results are the average of three repeated measurements for all samples.

**Contact angle** was determined on paper sheets using a video contact angle system (Krüss DSA 25B, Germany). The average surface hydrophilicity was obtained via applying water droplets on each paper sheet surface at five different locations.

## RESULTS AND DISCUSSION

### Characterization of the prepared ($TiO_2/SiO_2$) core-shell pigments

#### *X-ray diffraction*

According to the XRD pattern in Figure 2, silica typically exhibits an amorphous nature. However, the introduction of titanium dioxide at low concentration, in the range of 10-20%, of the whole core-shell structure, which represents the shell that covers the surface of the silica, resulted in a significant transformation to the crystalline form, as verified by the sharp and intense peaks representing the anatase phase of titanium dioxide, with its significant peaks corresponding to 2-theta positions at 31.2°, 36.9°, and 55.1°, in accordance with JCPDS card no. 21-1272.

#### *X-ray fluorescence*

The results of XRF analysis for the three prepared pigments, along with silica fume, indicated that the concentration of titanium dioxide was increased in ascending order from $TiO_2/SiO_2$ (1) to $TiO_2/SiO_2$ (3), which do not exceed 10-20% of the core-shell structure, and accordingly the percentage of silicon dioxide in the core-shell pigments was decreased, signifying the replacement of titanium dioxide to a portion of the silicon dioxide in the surface. This led to the production of the core-shell particles with silica acting as the core and titanium dioxide serving as the shell. Hence, silica is still the dominant component in all of the three pigments, representing 80-90% of the whole compound, and this is clear from the results in Table 1.

#### *Scanning and transmission electron microscopy*

Figures 3 and 4 illustrate the morphology of the prepared pigments, as observed through SEM and TEM techniques. The images emphasize the distinct characteristics of both silica fume and titanium dioxide particles; with the appearance of silica fume as spherical particles with various sizes, ranging from 2-15 µm, as can be seen in the TEM photos. In addition, titanium dioxide was observed in very small sized plates integrated or deposited on the surface of the silica spheres; these different shapes were overlapping each other and cannot be separated, confirming the preparation of the new core-shell pigments.

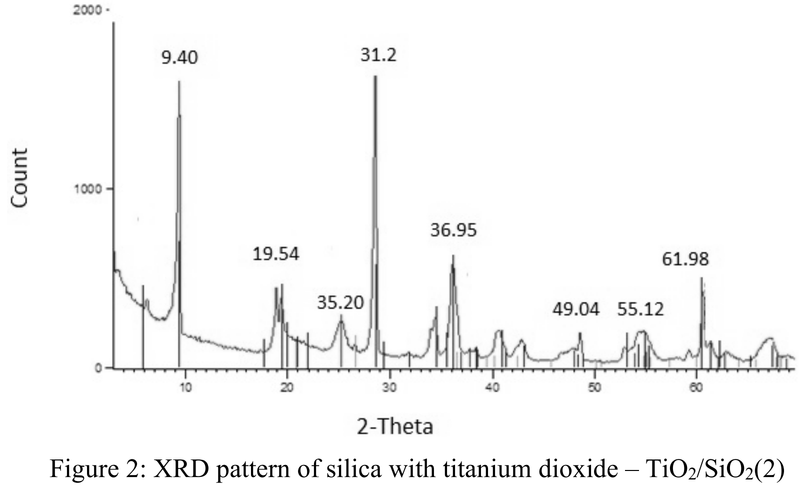

Figure 2: XRD pattern of silica with titanium dioxide – $TiO_2/SiO_2$(2)

Table 1
XRF of silica fume and silica covered with titanium dioxide

| Main constituents (wt%) | Silica | $TiO_2/SiO_2(1)$ | $TiO_2/SiO_2(2)$ | $TiO_2/SiO_2(3)$ |
|---|---|---|---|---|
| $SiO_2$ | 95.0 | 93.3 | 92.5 | 91.02 |
| $TiO_2$ | -- | 2.7 | 4.9 | 5.6 |
| MgO | 1.02 | 0.95 | 0.94 | 0.85 |
| $Al_2O_3$ | 0.003 | 0.021 | 0.23 | 0.22 |
| $Fe_2O_3$ | 1.2 | 1.09 | 1.18 | 1.12 |
| MnO | 0.06 | 0.027 | 0.030 | 0.26 |
| CuO | -- | -- | 0.006 | 0.004 |
| NiO | -- | 0.006 | 0.006 | 0.006 |
| CaO | 0.62 | 0.40 | 0.60 | 0.48 |
| $K_2O$ | 0.29 | 0.65 | 0.71 | 0.63 |
| $P_2O_5$ | 1.10 | 0.08 | 0.02 | 0.01 |
| $SO_3$ | 0.044 | 0.25 | 0.37 | 0.36 |
| Cl | 0.03 | 0.05 | 0.05 | 0.02 |

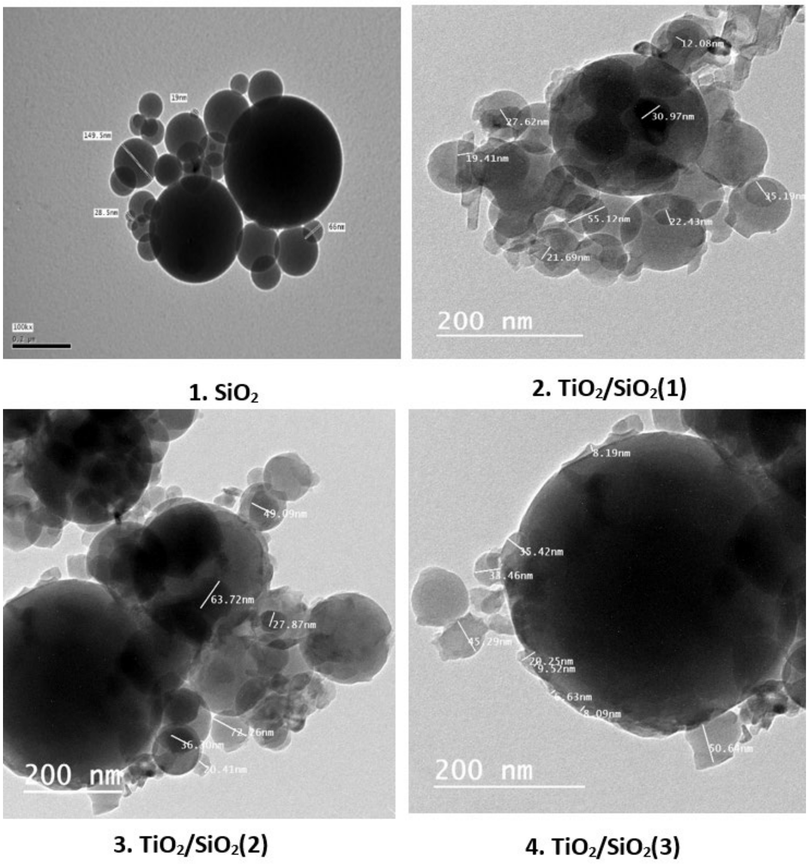

**1. $SiO_2$**　**2. $TiO_2/SiO_2(1)$**

**3. $TiO_2/SiO_2(2)$**　**4. $TiO_2/SiO_2(3)$**

Figure 3 TEM images of silica fume and $TiO_2/SiO_2$ core-shell pigments

This was predominantly evident in the SEM images in Figure 4, showing a background of clusters with fine, high-purity silica particles integrated with small and randomly distributed plates of titanium dioxide. This combined morphology of sphere and plate structures engaged a crucial role in reinforcing the films with excellent strengthening properties that can effectively delay the penetration of water vapor to the paper surface, leading to reduced water and gas permeability. This topic will be further discussed below.

### *EDX analysis*

Figure 4 presents the results of the EDX analysis of the prepared pigments. EDX, or energy dispersive X-ray analysis, is capable of detecting elements on the surface up to a depth of one micron. The chart clearly indicated the presence of titanium, silicon and oxygen elements, with the domination of silica (43.47%). The peaks also indicated the presence of titanium dioxide on the surface of silica in concentration not exceeding 10%. According to XRF analysis, which gives an idea about the bulk concentration of the elements, followed by the EDX, which indicates the elements on the surface, it is now appropriate to tell that the core-shell pigments are formed successfully, with a silica core and titanium dioxide shell, which does not exceed 10-20%.

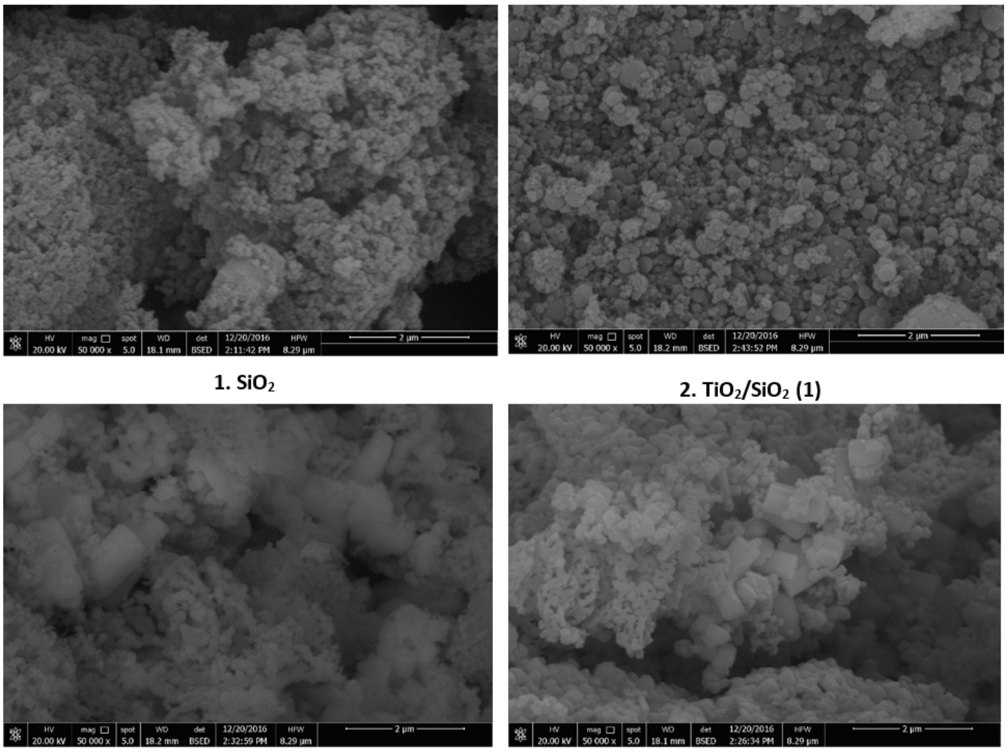

1. $SiO_2$ 2. $TiO_2/SiO_2$ (1)

3. $TiO_2/SiO_2$(2) 4. $TiO_2/SiO_2$(3)

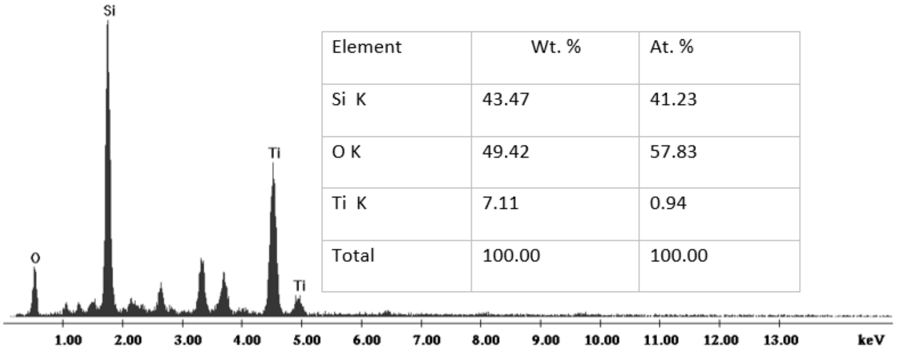

| Element | Wt. % | At. % |
|---|---|---|
| Si K | 43.47 | 41.23 |
| O K | 49.42 | 57.83 |
| Ti K | 7.11 | 0.94 |
| Total | 100.00 | 100.00 |

Figure 4: SEM/EDX images of silica fume and $TiO_2/SiO_2$ (3) core-shell pigments

## Characterization of coated paper sheets

### *Strength properties of coated paper sheets*

An increase in the weight gain of paper sheets coated with $TiO_2/SiO_2$ core-shell pigments was perceived, compared to that of unmodified blank and neat PLA, as shown in Figure 5. Paper bulk density describes the relation between the thickness of paper and its grammage, the results exemplified in Figure 6(a) display an indirect relationship between the bulk density of the modified paper sheets and the loading of $TiO_2/SiO_2$. The pigment particles tend to fill the gaps between fibers, which are bonded tightly together in the sheet. Paper strength is dependent on the extent of bonding of the fibers to each other (interfiber bonding) and their distribution within the sheet. This bonding first starts from the formation of hydrogen bonds between fibers; and paper strength is dependent on the fiber contact area and its intrinsic strength per unit area.

It is widely accepted that using mineral fillers in paper-making leads to a striking reduction in paper strength, and it can be evident in two aspects.[26] First, mineral fillers can interfere with fiber-to-fiber bonding due to the poor bond abilities of filler matrices. Second, the replacement of fibers by pigments usually leads to reducing the amount of fibers in the paper matrix, affecting negatively its strength. Figure 6 displays the results of tensile strength, tensile index, breaking length, maximum load and Young's modulus tests.

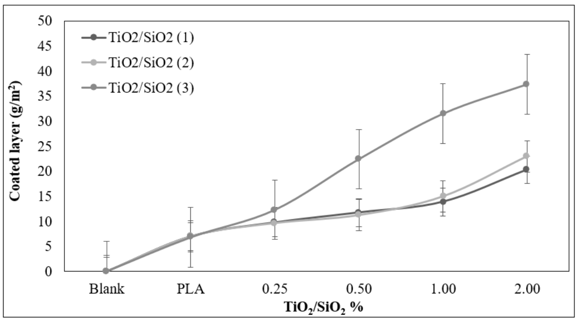

Figure 5: Weight gain of bleached bagasse paper sheets coated with PLA-$TiO_2/SiO_2$

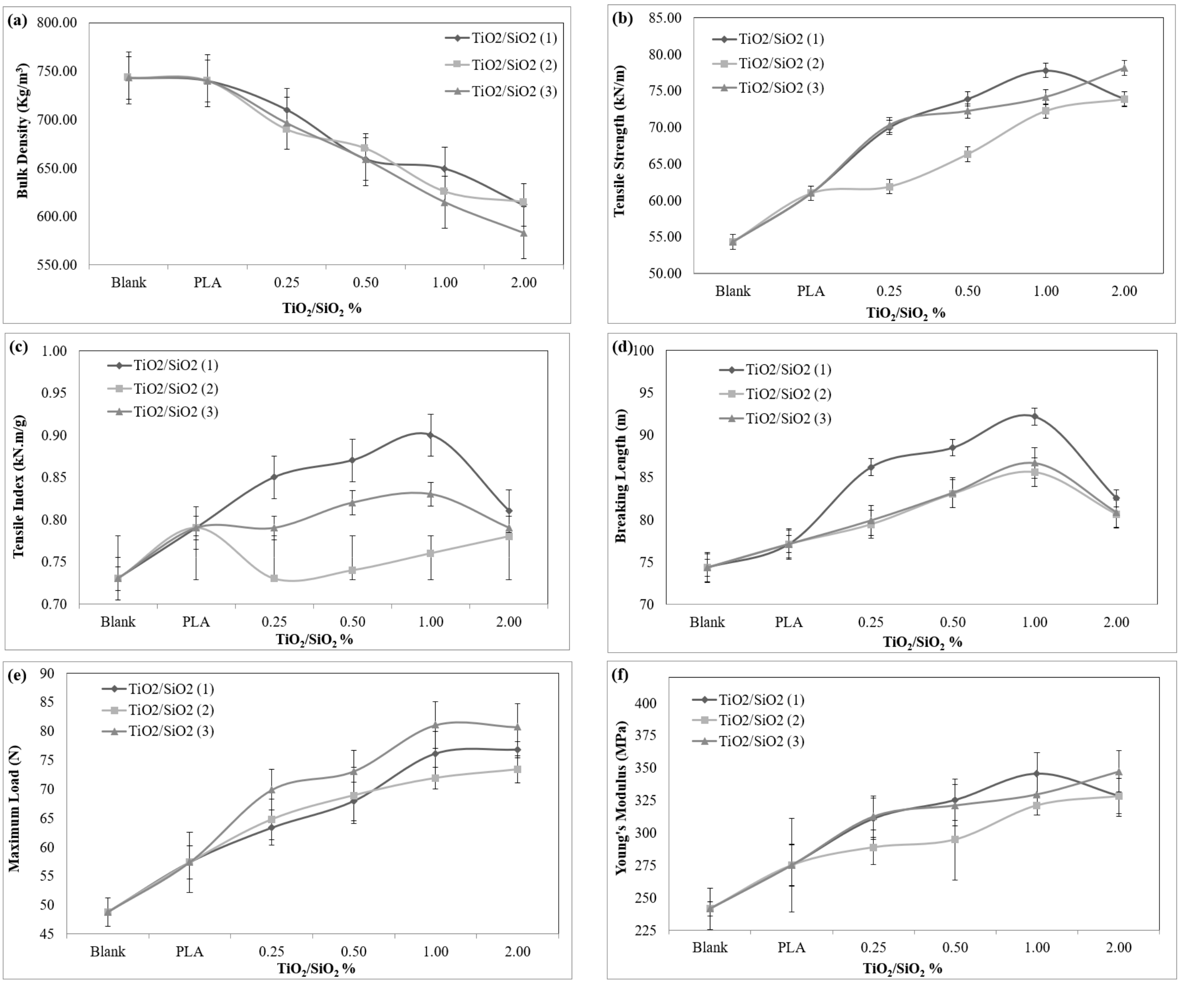

Figure 6: Mechanical properties of bleached bagasse paper sheets treated with PLA-$TiO_2/SiO_2$

Tensile strength is considered as the most basic property of packaging materials that can give an indication of the paper ability to resist breaking under tension. This breaking is dependent on the surface area of fibers, their length and strength, and on their bonding strength. Adding PLA-$TiO_2/SiO_2$

(1) and PLA-$TiO_2/SiO_2$ (3) led to an increase in the tensile strength of coated paper sheets, which reached 78.12 ±1.00kN/m for 2% PLA-$TiO_2/SiO_2$ (3) concentration, compared to the blank paper sheet, which had 54.34 ± 1.00kN/m. As shown in Figure 6 (b and c), tensile strength presented an improvement in the case of coated paper sheets with films containing $TiO_2/SiO_2$ (1) and $TiO_2/SiO_2$ (3), with an improvement reaching 43.14% and 43.76% with concentrations of 1% and 2%, respectively.

As shown in Figure 6 (d, e and f), breaking length, maximum load and Young's modulus offered the same improvement results for paper sheets coated with different concentrations of $TiO_2/SiO_2$ (1), $TiO_2/SiO_2$ (2) and $TiO_2/SiO_2$ (3), ranging between 0.25%-2%, besides the maximum increment at 1% concentration for the three core-shell pigments. As shown, the improvement in strength property of the paper sheets was enhanced in the case of coated papers with PLA-$TiO_2/SiO_2$, which is related to the good dispersion of the core-shell pigment in the cellulosic matrix. The maximum improvement was realized in the case of papers coated with PLA- $TiO_2/SiO_2$(1) due to the higher binding between paper sheet fibers, which can be explained by the presence of hydroxyl groups of silicates and $TiO_2$, which can promote better bonding not only between $TiO_2/SiO_2$ and cellulose fibers, but also between the fibers themselves. Hydrogen bonding was formed between PLA and $TiO_2/SiO_2$ core-shell particles, PLA and cellulose fibers, cellulose fibers and $TiO_2/SiO_2$ pigment and also among the cellulose fibers. This extra-binding among the fibers can increase their adhesion and consequently can enhance their mechanical properties.

## Barrier properties of coated paper sheets

### *Water vapor permeability*

The water vapour permeability (W/V) of modified paper was measured through identifying the volume of water moving through the paper matrix per unit area and time under specific conditions. The WVP of composite films presented in Figure 7 revealed that paper sheets treated with $TiO_2/SiO_2$ core-shell pigments showed a gradual decrease in the water vapour permeability with the increase in the pigment content, compared to the blank and the coat containing neat PLA. This behavior might be due to the changes in the porosity of paper and the hydrophobic properties of the coating film, which prevented water from penetrating the paper network. In comparison with paper coated with $TiO_2/SiO_2$ (2) and $TiO_2/SiO_2$ (3), those coated with $TiO_2/SiO_2$(3) offered lower hydrophobicity, as clarified in Figure 7. Films containing neat PLA showed WVP of $3.24\times10^{-6}$ g.cm.h.kPa, which decreased significantly after its mixing with $TiO_2/SiO_2$ core-shell pigments. Among the composite films, those containing PLA-$TiO_2/SiO_2$(3) and PLA-$TiO_2/SiO_2$(2) displayed the lowest WVP of $1.36\times10^{-6}$g.cm.h.kPa at 2% concentration. The decrease in the WVP of the composite films was due to the more tortuous path of water vapor created by the impermeable pigments with their different concentrations. In addition, the WVP of $TiO_2/SiO_2$ core-shell pigments can be attributed to various factors, such as the type of biopolymers, compatibility between the biopolymer matrix and the pigments, and the pigment concentration. $TiO_2/SiO_2$ core-shell pigments partially locked the cellulosic pores in the matrix through the formation of a homogenous layer on the surface, as displayed in the SEM images in Figure 10, due to their lower porosity.

### *Contact angle*

Measuring the contact angle of the water droplet on paper sheets coated with varying PLA-$TiO_2/SiO_2$ composite films made it possible to investigate the effect of both PLA and PLA-$TiO_2/SiO_2$ on the surface hydrophilicity of the sheets. Figure 8 confirms that applying PLA, with its hydrophobic nature, in the coating on the paper sheet surfaces caused the contact angle to rise from 38.8 to 86.7°. However, the contact angle decreased from 86.7° to 81.0°, 75.5°, and 81.8° in the case of coatings containing $TiO_2/SiO_2$ core-shell pigments at the concentration of 2%, due to their hydrophilic nature. This can be attributed to the presence of (-OH) groups that adsorb water molecules in the pigment structure, creating PLA films that are more hydrophilic. This is in line with the pigments' natural hydrophilicity, which is confirmed by their low contact angle value. Accordingly, adding $TiO_2/SiO_2$ pigments in the coat of the paper sheets caused a decrease in the hydrophobicity of the sheets, but it is still significantly higher than that of uncovered paper sheets, which is consistent with the previously discussed WVP and water absorption results.

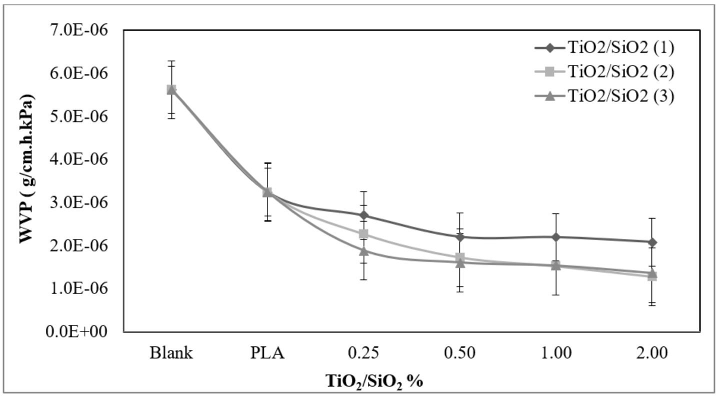

Figure 7: Water vapor permeability of bleached bagasse paper sheets treated with PLA-$TiO_2/SiO_2$

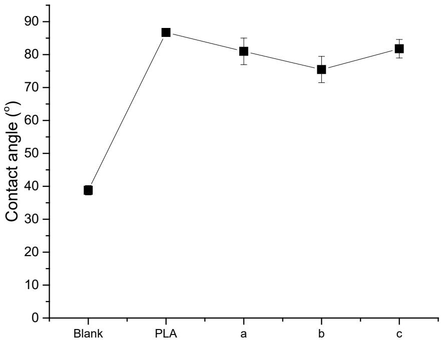

Figure 8: Water contact angle of blank (untreated paper) and paper coated with PLA, (a) PLA-2% $TiO_2/SiO_2$(1), (b) PLA-2% $TiO_2/SiO_2$(2) and (c) PLA-2% $TiO_2/SiO_2$(3)

### *ATR-FTIR analysis*

The ATR-FTIR spectra of uncoated paper and paper coated with PLA and $TiO_2/SiO_2$ (3) (1% and 2%) are shown in Figure 9. The spectrum of the uncoated paper sheet presented the distinctive absorption peaks associated with cellulose. Specifically, it exhibited a strong absorption band between 3600 and 3100 $cm^{-1}$, which is linked to the stretching of the O-H bond in the hydroxyl groups of cellulose. Also, a peak indicating the presence of interfacial or adsorbed water in the cellulose structure appeared at 1645 $cm^{-1}$. The absorption observed in the 3000 to 2800 $cm^{-1}$ range can be ascribed to the stretching vibration of the C-H bonds. On the other hand, the absorption witnessed in the 1450 to 1350 $cm^{-1}$ range can be endorsed to the asymmetric and symmetric deformation of the $CH_2$ and C-H groups.[27] The absorption observed in the 1300-900 $cm^{-1}$ region indicates cellulose and it is characterized by its complexity and intensity. This absorption is mostly attributed to the stretching C-O-C (1060 $cm^{-1}$) and C-O (1028 $cm^{-1}$) bonds within the cellulose structure. These bands were influenced by inter- and intra-molecular hydrogen bonding, making it closely tied to alterations in the chemical surface groups.[28] Upon applying PLA and PLA-$TiO_2/SiO_2$ (3) with concentrations of 1% and 2% onto the paper sheet, a manifested change in the ATR-FTIR spectra was detected, characterized by a shift and decrease in intensity of the O-H absorption peaks, compared to the uncovered paper sheet. A stretching of O-H and a bending absorption peak displayed a shift towards shorter wavelengths and a substantial decrease in intensity. This result suggested a significant interaction occurring at the interface between the hydroxyl (-OH) groups of cellulose, PLA, and Ti-O/Si-O bonds in the case of the films containing $TiO_2/SiO_2$ (3).[29]

Upon increasing $TiO_2/SiO_2$ (3) loading, the strength of the peaks corresponding to C-OH stretching (1060 $cm^{-1}$) and C-O-C bending vibrations (1163 $cm^{-1}$) steadily decreased, compared to uncoated paper sheet. An analogous occurrence was distinguished for the C-H stretching vibration at a frequency of 2910 $cm^{-1}$. The presence of $TiO_2/SiO_2$ nanoparticles leads to the inhibition of the C–H in-plane stretching due to steric hindrance that initiated this phenomenon. According to Adel *et al.*,[4,14] the cellulose and $TiO_2$ have a strong connection, suggesting that the finer particles are more likely to remain intact within the paper sheets, improving their endurance. Paper sheets coated with $TiO_2/SiO_2$ (3) with pigment concentration of 1% and 2% revealed clear and wide absorption peaks associated with $TiO_2$. The absorption peaks observed between 800 and 400 $cm^{-1}$ resulted from $TiO_2$ and $SiO_2$ particles, while the peaks between 750 and 600 $cm^{-1}$ were attributed to the stretching vibrations of Ti-O-Ti and Si-O-Si.[30] Another notice was detected for the C=O absorption band with little shifting in its positions and increase in the intensity after the integration of $TiO_2/SiO_2$ into PLA.

In the case of the PLA polymer, the carbonyl group (C=O) is the key functional group, which appeared at 1755 $cm^{-1}$ with low intensity. On the other hand, incorporating $TiO_2/SiO_2$ core-shell pigment into the PLA made the interactions between the polymer and the pigment to shift slightly in the C=O absorption band in the FTIR spectrum to become at 1752 and 1751 $cm^{-1}$ for 1% and 2% $TiO_2/SiO_2$ (3), respectively, with increased intensity. Different assumptions can explain this increase in the intensity and the shift of the peak. First, the carbonyl group in PLA can form hydrogen bonds with the hydroxyl groups (-OH) present on the surface of the $TiO_2/SiO_2$ core-shell pigment. These hydrogen bonding interactions can alter the electronic environment around the carbonyl group, leading to a shift in the C=O absorption band. Another assumption suggests that the carbonyl group in PLA has a partial positive charge on the carbon atom and a partial negative charge on the oxygen atom, creating a dipole moment. The $TiO_2/SiO_2$ core-shell pigment may also have dipole moments, and the interactions between these dipoles can affect the C=O absorption band.

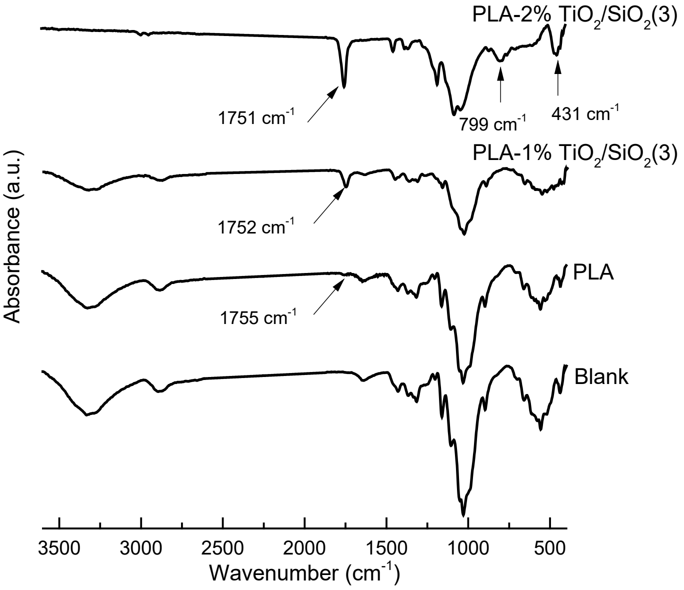

Figure 9: ATR-FTIR spectra of uncoated paper and paper coated with PLA, PLA-1% $TiO_2/SiO_2$(3), and PLA-2% $TiO_2/SiO_2$(3)

***Surface morphology***

Figure 10 displays the change in the surface morphology of uncoated and coated paper sheets with films containing $TiO_2/SiO_2$ core-shell pigments and PLA. The deposition of PLA and PLA-$TiO_2/SiO_2$ showed a great effect on the surface chemistry of the fibers and then on its network. The formed film characteristics of the paper sheets were investigated using SEM. It can be clearly seen in Figure 10 (a) that unmodified paper showed a typical morphology of any normal paper, which is a fiber network with free pores and randomly distributed fibers. After treating with PLA, as displayed in Figure 10 (b), the free pores became relatively smooth, compact and the surface properties of paper sheets were improved. Adding PLA-$TiO_2/SiO_2$ core-shell particles led to a slightly rough surface, with more effective adherence and bonding to the surface of the fiber matrix, leading to the enhancement of the chemical compatibility with the cellulosic fibers and better cross-linking with cellulosic matrix (Fig. 10 (c)).

From the results, it is clear that $TiO_2/SiO_2$ core-shell particles are well dispersed in the cellulosic fiber, but with a tendency of aggregation. This tendency can be attributed to the fact that no surface treatment was performed on the oxide particles, and the preparation of PLA-$TiO_2$/$SiO_2$ was done through solution mixing via the direct dispersion of $TiO_2$/$SiO_2$ particles in PLA solution. This dispersion can directly affect the physical properties of PLA-$TiO_2$/$SiO_2$ and paper matrix, but this effect was overcome by the extraordinary properties of the tailored core-shell particles.[31]

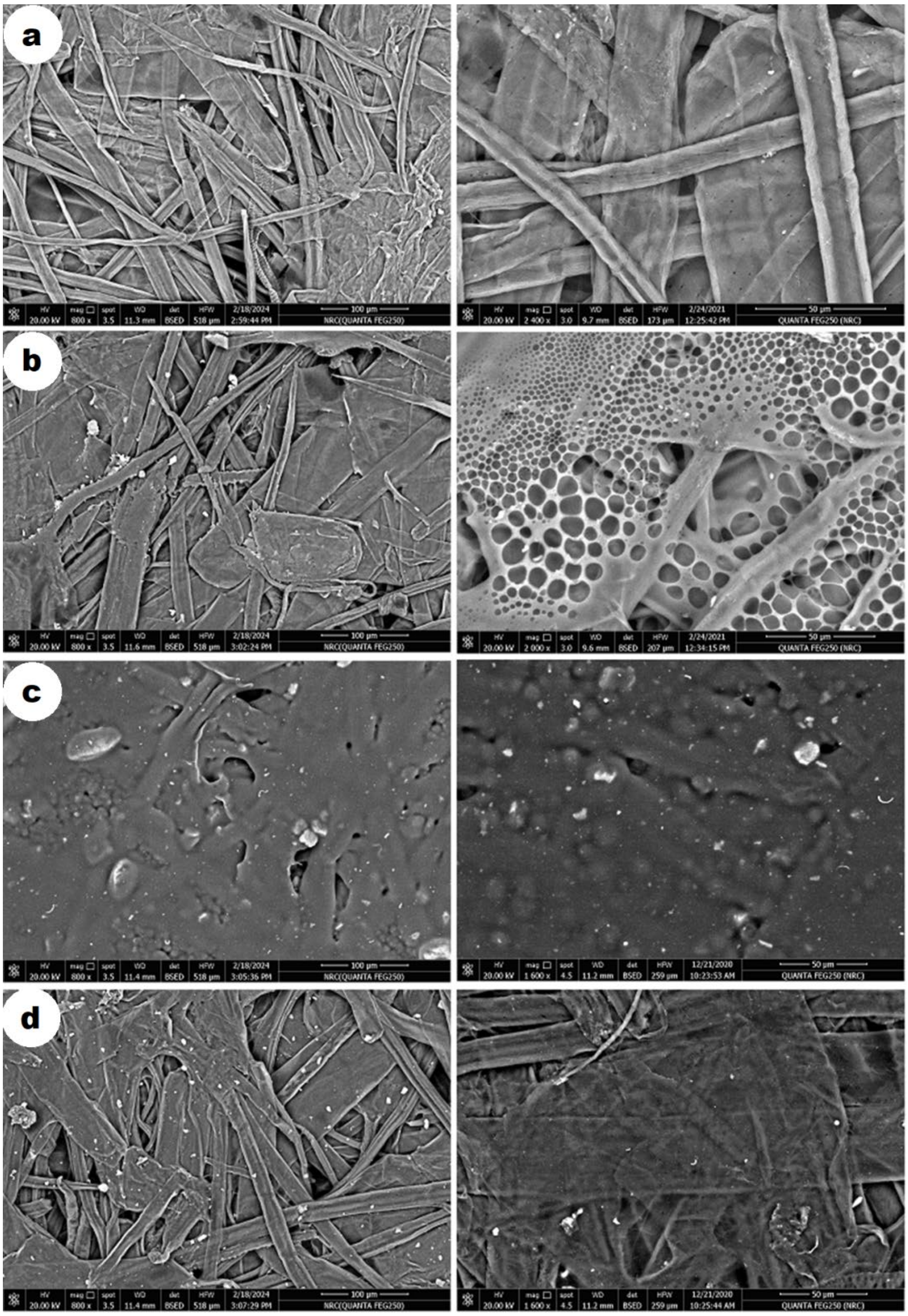

Figure 10: SEM surface micrographs of (a) untreated paper and paper coated with (b) PLA, (c) PLA-1% $TiO_2$/$SiO_2$(3), and (d) PLA-2% $TiO_2$/$SiO_2$(3) at two magnifications 800x (left) and ≈1600x (right)

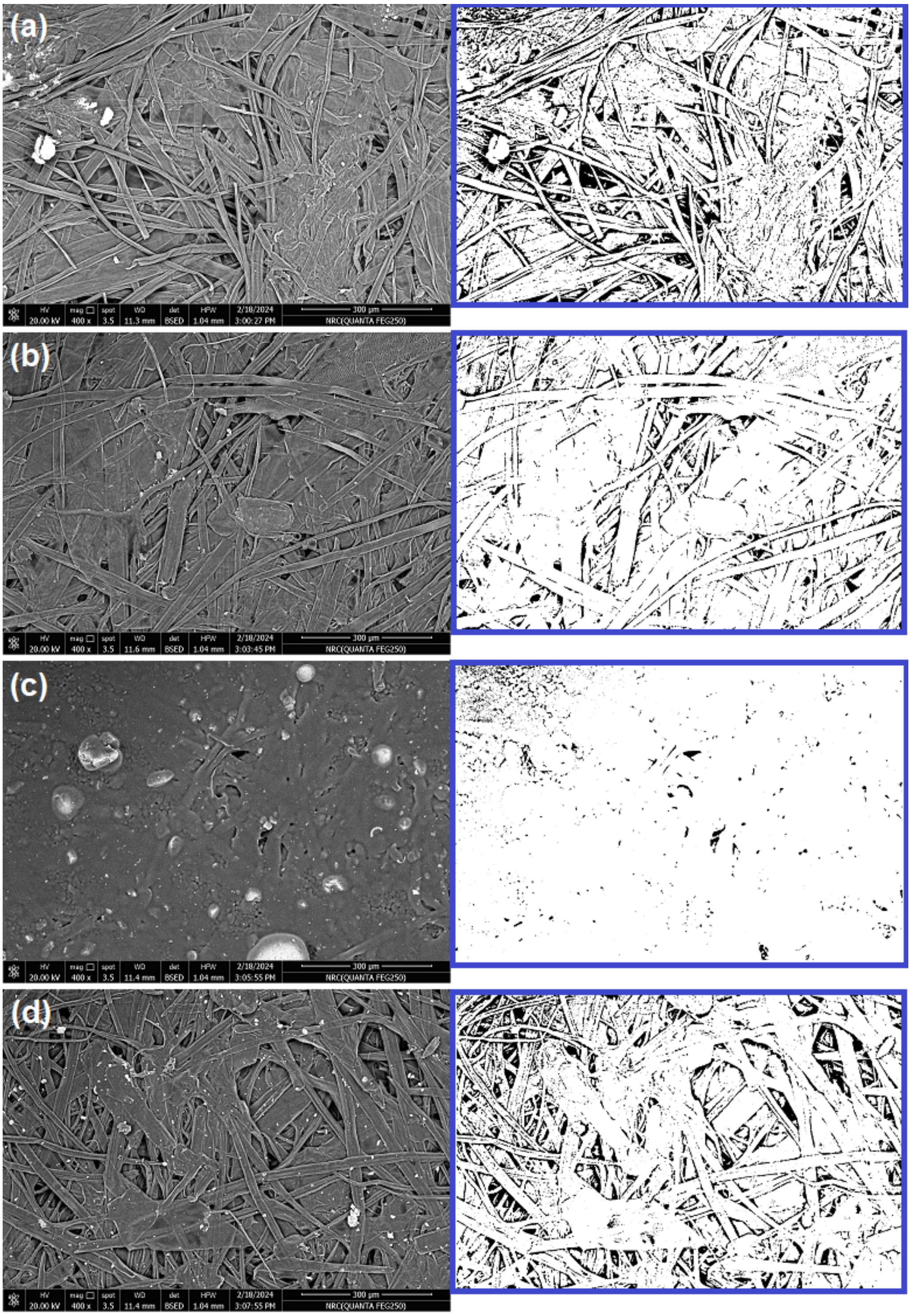

Figure 11: Original SEM images at 400x magnification and the corresponding binary image filling holes for (a) untreated paper, and paper coated with (b) PLA, (c) PLA-1% $TiO_2/SiO_2$(3), and (d) PLA-2% $TiO_2/SiO_2$(3)

According to Cui, Huang, and Liu, porosity, which is defined as the empty space between a substance and a tiny portion of vacant volume space within the entire volume, is a crucial physical property that can indicate texture and material quality characteristics.[32] The porosity value is in opposition to the fluid content of the material that is decisive for the production of paper. Porosity can be defined mathematically as the difference between the volume of pores and the total volume of the material.[33] The difference between the original images and binary ones are presented in Figure 11; it is obvious that as the area of the air cavity of the paper was smaller, detected by the smaller paper pores, better barrier properties can be attained, due to the small pores that can lead to lower water vapor uptake. Uncoated and coated paper sheets with coatings containing PLA-1% $TiO_2/SiO_2$ (3) offered the lowest porosity, as can be seen in Table 2, which is in high agreement with the outcomes of water adsorption and WVP tests. Therefore, the optimum concentration of core-shell pigments recommended for use in the coating containing PLA/$TiO_2/SiO_2$ (3) was 1%, this being the best coating composition on paper sheets.

Table 2
Porosity data for uncoated and coated paper sheets with PLA, PLA-1% $TiO_2/SiO_2$(3), and PLA-2% $TiO_2/SiO_2$(3)

| Sample | Total area, μm$^2$ | Average size, μm | Porosity, % | Feret diameter, μm |
|---|---|---|---|---|
| Blank | 120746.9 | 168.406 | 17.153 | 29.833 |
| PLA | 57994.36 | 101.923 | 8.215 | 24.779 |
| 1% $TiO_2/SiO_2$(3) | 8024.952 | 57.321 | 1.139 | 14.85 |
| 2% $TiO_2/SiO_2$(3) | 106041.8 | 171.312 | 15.045 | 27.749 |

Feret's diameter is the longest distance between any two points along the selection boundary, also known as maximum caliper

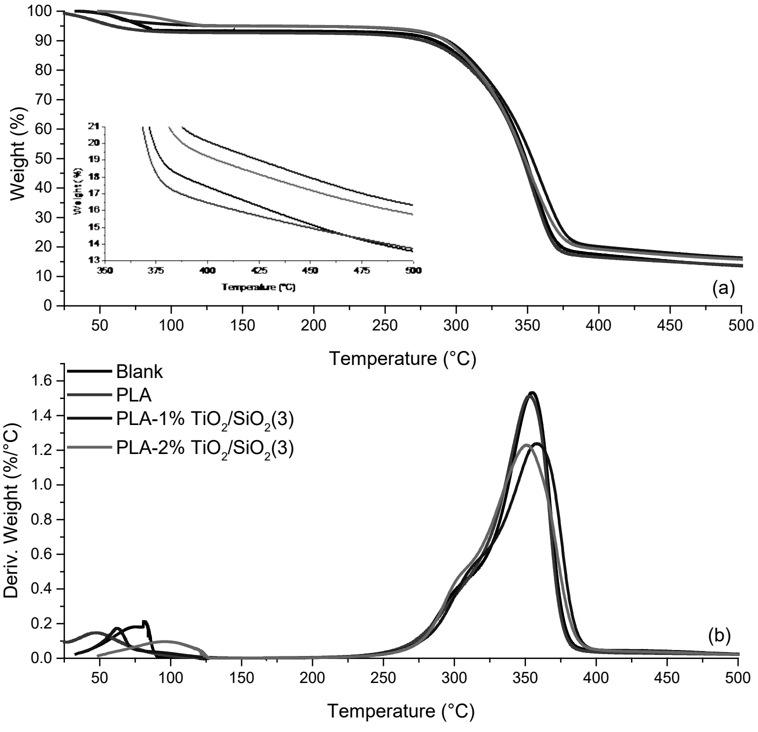

Figure 12: TGA and DTG curves of untreated paper and paper coated with PLA, and PLA-1% $TiO_2/SiO_2$(3), and PLA-2% $TiO_2/SiO_2$(3)

### *Thermogravimetric analysis*

Thermogravimetric analyses were performed in a nitrogen atmosphere to examine the thermal stability of uncoated and coated paper sheets. Figure 12 exemplified the comparatively low temperature at which different paper sheets decompose. The corresponding weight loss (TG) and the first derivative curve (DTG) of uncoated paper sheets showed that the cellulosic fiber typically went through a single main stage of heat degradation in nitrogen. The moisture evaporated from the sample at the onset of heating explained the slight weight loss at temperatures below 100 °C. In the case of uncoated paper sheets, the primary decomposition phase comprised two overlapping pyrolysis stages at higher temperatures. In the first stage, hemicelluloses breakdown ensues, overlapping with the second stage of pyrolysis of the primary cellulose component. At this point, levoglucosan, which is a byproduct of burning cellulose, was formed as an end-product.[34]

Table 3
Thermo-analytical and thermodynamic data of thermal decomposition of paper sheets coated with PLA-$TiO_2/SiO_2$

| Sample | Phase | $T_o$ | $T_m$ | WL, % | $WLR_{max}$, %·min/°C | Ea, kJ/mol | A, 1/s | ΔHa, kJ/mol | ΔSa, J/K mol | ΔGa, kJ/mol |
|---|---|---|---|---|---|---|---|---|---|---|
| Blank | 1 | 40 | 81.14 | 7.50 | 6.828 | 83.82 | $7.06X10^{11}$ | 80.87 | -19.51 | 87.78 |
| | 2 | 315.32 | 355.03 | 79.09 | | 151.52 | $5.65X10^{11}$ | 146.30 | -26.14 | 162.71 |
| | | | | | | ∑235.33 | | ∑227.17 | ∑-45.65 | ∑250.49 |
| PLA | 1 | 40 | 49.28 | 8.35 | 6.964 | 28.66 | $1.99X10^{3}$ | 25.98 | -182.47 | 84.78 |
| | 2 | 310.5 | 352.96 | 78.02 | | 143.60 | $1.19X10^{11}$ | 138.40 | -39.05 | 162.84 |
| | | | | | | ∑172.26 | | ∑164.37 | ∑-221.52 | ∑247.62 |
| 1% $TiO_2/SiO_2$(3) | 1 | 40 | 62.41 | 6.09 | 4.497 | 47.14 | $1.14X10^{6}$ | 44.35 | -129.95 | 87.94 |
| | 2 | 306.79 | 358.09 | 77.69 | | 139.07 | $3.78X10^{10}$ | 133.83 | -48.67 | 164.54 |
| | | | | | | ∑186.21 | | ∑178.17 | ∑-178.62 | ∑252.48 |
| 2% $TiO_2/SiO_2$(3) | 1 | 40 | 95.61 | 5.27 | 4.665 | 60.61 | $3.36X10^{7}$ | 57.55 | -102.63 | 95.38 |
| | 2 | 295.3 | 350.82 | 80.35 | | 148.57 | $2.88X10^{11}$ | 143.38 | -31.68 | 163.14 |
| | | | | | | ∑209.18 | | ∑200.93 | ∑-134.30 | ∑258.52 |

The TG curve of functionalized sheets with PLA and $TiO_2/SiO_2$ (3) with concentration of 1% and 2% experienced weight loss below 125 °C that ranged from 5.27 to 8.35%, resulting from absorbed moisture loss of the sheets. The DTG curve of coated paper sheets displayed a single peak of breakdown with a left-hand shoulder, resembling that of the uncoated paper sheet. Owing to the early breakdown of the coating containing PLA on the surface of the cellulose fibers, a shift occurred in the temperature at which degradation begins and reached its most significant weight loss. Approximately 78.02, 77.69, and 80.35% of the weight from coated papers with coatings containing PLA, 1% $TiO_2/SiO_2$ (3), and 2% $TiO_2/SiO_2$ (3), respectively, was apparent. The paper treated with neat PLA and $TiO_2/SiO_2$ (3) at 1 and 2% showed a similar degradation pattern to the blank sample. The TG thermogram revealed that paper covered with PLA lost weight by approximately 78.02% between 225 °C and 385 °C as the carbon species in the composites were burnt. The DTG curve revealed a maximum weight loss rate ($WLR_{max}$) of 6.964% min/°C, surpassing the rates of uncoated sheets and papers coated with $TiO_2/SiO_2$ (3) films. Therefore, the faster rate of weight loss ($WLR_{max}$) suggested that paper coated with PLA disclosed lower thermal stability. Contrariwise, adding $TiO_2/SiO_2$(3) at 1 and 2% to the coating mixture decreased the $WLR_{max}$ value to 4.497 and 4.665% min/°C, respectively, with rather higher CR% of 16.3 and 15.8%.

Using Coats and Redfern's theory, TG analyses and pseudo-first-order kinetics were used to find the thermodynamic and kinetic parameters for the main stage of decomposition, including pre-exponential factors (A), activation energies (Ea), Gibbs free energy of activation ($\Delta Ga$), entropy ($\Delta S$), and enthalpy ($\Delta H$), all included in Table 3. Coated papers with films containing PLA and 1% $TiO_2/SiO_2$ (3) showed lower Ea and A than uncoated papers and those coated with films containing 2% $TiO_2/SiO_2$ (3) core-shell pigment. This might be due to the low energies required to trigger the pyrolysis processes caused by the presence of PLA and 1% $TiO_2/SiO_2$ (3) pigment in the coating covering the cellulose fibers. As a result, integrating $TiO_2/SiO_2$ (3) in the PLA coating covering the paper sheets altered the pyrolysis reaction pathway, causing a decrease in the activation energy.

Normally, using Gibbs free energy showed the difference between the reactant and activated state energies, for thermal reactions, to assess this process's spontaneity. Consequently, the obtained positive G values showed that the heat degradation of uncoated and coated paper sheets is not spontaneous. In addition, the entropy and enthalpy values are commonly negative and positive in thermal reactions, respectively. The negative enthalpy values indicated an endothermic state between the activated complex and the reactant, resulting in increased degradation with rising temperatures.[35] On the other hand, the negative entropy values demonstrated less structural freedom in the transition state than in the reactant. Accordingly, the data presented in Table 3 established that the thermal stability of the coated paper sheets did not deteriorate during the coating treatment. Otherwise, the preceding discussion could suggest thermal improvements after covering the paper sheets with films containing PLA-$TiO_2/SiO_2$ (3).

## CONCLUSION

In this work, a new core-shell pigment ($TiO_2/SiO_2$) based on silica fume waste covered with a thin layer of $TiO_2$ combined with PLA was used as a coating for paper sheets. This core-shell pigment was prepared with three different concentrations of $TiO_2$ as the shell to estimate the role of this system and the effect of the shell thickness on different properties of the paper. The following conclusions have been drawn:

- The incorporation of PLA-$TiO_2/SiO_2$ with different concentrations in the fiber matrices improved the tensile strength, especially in the case of coated paper sheets with films containing $TiO_2/SiO_2$ (1) and $TiO_2/SiO_2$ (3); this change in the tensile strength reached 43.14% and 43.76% with concentrations of 1% and 2%, respectively. The network created by the PLA film blended with the ($TiO_2/SiO_2$) pigments on paper sheet substrate was highly dense and organized, causing the creation of a smooth distribution of the pigment particles that filled the pores in the paper matrices and increased the water vapor resistance of the samples coated with $TiO_2/SiO_2$ pigments, compared to the blank (uncoated paper).
- The coatings containing PLA only and PLA-$TiO_2/SiO_2$ revealed WVP of $3.24\times10^{-6}$ g.cm.h.kPa, and this value decreased

significantly after mixing with $TiO_2/SiO_2$ core-shell pigments, demonstrating a significant positive effect on the surface chemistry of the paper fibers and on their networks.

- Also, applying PLA with its hydrophobic nature in the coating to cover the surface of the paper sheet caused the contact angle to rise from 38.8 to 86.7°. However, the contact angle decreased from 86.7° to 81.0°, 75.5°, and 81.8° in the case of coatings containing $TiO_2/SiO_2$ core-shell pigments at the concentration of 2%, due to their hydrophilic nature.
- The surface morphology of coated paper sheets also displayed that adding $TiO_2/SiO_2$ core-shell particles led to a slightly rough surface, with more effective adherence and bonding to the surface of the fiber matrix, leading to the enhancement of their chemical compatibility with the cellulosic fibers and better cross-linking with the cellulosic matrix. Uncoated and coated paper sheets with films enclosing PLA-1% $TiO_2/SiO_2$ (3) offered the lowest porosity, which is in high agreement with the outcomes of water adsorption and WVP tests. Therefore, it can be concluded that the optimum concentration of core-shell pigments recommended the use in coatings containing PLA-$TiO_2/SiO_2$ (3) is 1%, which was established as the best coating composition for paper sheets.
- Coating paper with biopolymers, such as polylactic acid, still has limited applicability in the packaging sector, because of their drawback in lowering the mechanical and barrier capabilities, while their high manufacturing costs, relative to existing petroleum-based polymers, are hindering commercialization on an industrial scale. To develop cost-effective coating materials, it will therefore be better to use biopolymer blends, based on blending biopolymers with fillers, plasticizers *etc*. Finally, PLA-$TiO_2/SiO_2$ coated papers were evaluated for packaging and the measurements confirmed that the coated papers demonstrated an improvement in the tensile strength, water vapor resistance and hydrophobic property, compared with uncoated samples. These findings suggest that PLA-$TiO_2/SiO_2$ coated paper would be a suitable candidate for an environmentally friendly and functional packaging material.

***ACKNOWLEDGEMENTS***: All authors would like to thank the National Research Center (NRC), Egypt, for its financial support.

## REFERENCES

[1] M. Adel, N. M. Ahmed, M. A. Diab, F. N. El-Shall and N. El-Shinnawy, *Sci. Rep*., **13**, 6536 (2023), https://doi.org/10.1038/s41598-023-33546-9

[2] V. Alirach, M. Lubwama, P. W. Olupot and L. Kukunda, *Biomass Convers. Biorefin*., 1 (2023), https://doi.org/10.1007/s13399-023-04689-6

[3] A. M. Adel, E. O. Ahmed, M. M. Ibrahim, W. K. El-Zawawy and A. Dufresne, *Ind. Crop. Prod*., **93**, 175 (2016), https://doi.org/10.1016/j.indcrop.2016.04.042

[4] R. G. Toro, M. Diab, T. de Caro, M. Al-Shemy, A. Adel *et al*., *Materials*, **13**, 1326 (2020), https://doi.org/10.3390/ma13061326

[5] F. Jahangiri, A. K. Mohanty and M. Misra, *Green Chem*., **26**, 4934 (2024), https://doi.org/10.1039/D3GC02647G

[6] A. M. Adel, N. M. Ahmed, M. A. Diab and M. M. Selim, *Powder Technol*., **291**, 437 (2016), https://doi.org/10.1016/j.powtec.2016.01.007

[7] A. El-Gendy, M. El-Sakhawy, A. M. Adel and M. T. Al-Shemy, *Cellulose Chem. Technol*., **54**, 993 (2020), https://doi.org/10.35812/CelluloseChemTechnol.2020.54.96

[8] N. G. Khouri, J. O. Bahú, C. Blanco-Llamero, P. Severino, V. O. C. Concha *et al*., *J. Mol. Struct*., **2024**, 138243 (2024), https://doi.org/10.1016/j.molstruc.2024.138243

[9] T. R. P. Soares, A. F. Reis, J. W. S. dos Santos, E. G. L. Chagas, A. C. Venturini *et al*., *Food Bioproc. Tech*., **16**, 1101 (2023), https://doi.org/10.1007/s11947-022-02989-9

[10] P. Kumar, A. Kishore, S. Tripathi, V. Chaudhary and K. K. Gaikwad, *Biomass Convers. Biorefin*., 1 (2024), https://doi.org/10.1007/s13399-024-06066-3

[11] Y. Liu, X. Liang, S. Wang, W. Qin and Q. Zhang, *Polymers* (*Basel*), **10**, 561 (2018), https://doi.org/10.3390/polym10050561

[12] K. M. Lim, K. Z. Chiew, S. Y. Pung and W. S. Chow, *Mater. Today Proc*., **17**, 853 (2019), https://doi.org/10.1016/j.matpr.2019.06.372

[13] S. Shankar, L.-F. Wang and J.-W. Rhim, *Mater. Sci. Eng. C*, **93**, 289 (2018), https://doi.org/10.1016/j.msec.2018.08.002

[14] S. Feng, F. Zhang, S. Ahmed and Y. Liu, *Coatings*, **9**, 525 (2019), https://doi.org/10.3390/coatings9080525

[15] M. Connolly, Y. Zhang, D. M. Brown, N. Ortuño, M. Jordá-Beneyto *et al*., *Polym. Degrad. Stab*., **168**, 108938 (2019), https://doi.org/10.1016/j.polymdegradstab.2019.108938

[16] A. A. Singh, M. E. Genovese, G. Mancini, L. Marini and A. Athanassiou, *ACS Sustain. Chem. Eng*., 8, 4128 (2020), https://doi.org/10.1021/acssuschemeng.9b06760

[17] E. Gorgun, A. Ali and M. S. Islam, **9**, 11523 (2024), *ACS Omega*, https://doi.org/10.1021/acsomega.3c08448

[18] M. Ghozali, S. Fahmiati, E. Triwulandari, W. K. Restu, D. Farhan *et al*., *Polym.-Plast. Technol. Mater*., **59**, 1332 (2020), https://doi.org/10.1080/25740881.2020.1738475

[19] P. Beniwal, D. Guliani and A. P. Toor, *J. Polym. Res*., **31**, 68 (2024), https://doi.org/10.1007/s10965-024-03912-w

[20] A. M. Adel, F. N. El-Shall, M. A. Diab and M. T. Al-Shemy, *Biomass Convers. Biorefin*., **14**, 27905 (2024), https://doi.org/10.1007/s13399-022-03643-2

[21] M. Adel, M. T. Al-Shemy, M. A. Diab, M. El-Sakhawy, R. G. Toro *et al.*, *Int. J. Biol. Macromol*., **231**, 123270 (2023), https://doi.org/10.1016/j.ijbiomac.2023.123270

[22] S. Basak, M. S. Dangate and S. Samy, *Prog. Org. Coat*., **186**, 107938 (2024), https://doi.org/10.1016/j.porgcoat.2023.107938

[23] S. Feng, F. Zhang, S. Ahmed and Y. Liu, *Coatings*, **9**, 525 (2019), https://doi.org/10.3390/coatings9080525

[24] F. Cheng, M. Lorch, S. M. Sajedin, S. M. Kelly and A. Kornherr, *ChemSusChem*, **6**, 1392 (2013), https://doi.org/10.1002/cssc.201300305

[25] A. M. Adel, Z. H. Abd El–Wahab, A. A. Ibrahim and M. T. Al–Shemy, *Bioresour. Technol*., **101**, 4446 (2010), https://doi.org/10.1016/j.biortech.2010.01.047

[26] M. Çiçekler, T. Sözbir and A. Tutuş, *ACS Omega*, **8**, 21000 (2023), https://doi.org/10.1021/acsomega.3c01816

[27] M. D. Hosen, M. S. Hossain, M. A. Islam, A. N. M. A. Haque and M. Naebe, *J. Clean Prod*., **364**, 132665 (2022), https://doi.org/10.1016/j.jclepro.2022.132665

[28] D. Todorova, N. Yavorov and V. Lasheva, *Sustain. Chem. Pharm*., **27**, 100685 (2022), https://doi.org/10.1016/j.scp.2022.100685

[29] M. Ruzi, N. Celik and M. S. Onses, *Food Packag. Shelf Life*, **32**, 100823 (2022), https://doi.org/10.1016/j.fpsl.2022.100823

[30] B. Choudhury and A. Choudhury, *J. Lumin*., **132**, 178 (2012), https://doi.org/10.1016/j.jlumin.2011.08.020

[31] A. Buzarovska and A. Grozdanov, *J. Appl. Polym. Sci*., **123**, 2187 (2012), https://doi.org/10.1002/app.34729

[32] Z. Cui, Y. Huang and H. Liu, *J. Mech. Behav. Biomed. Mater*., **71**, 10 (2017), https://doi.org/10.1016/j.jmbbm.2017.02.014

[33] N. H. Astuti, N. A. Wibowo and M. Ayub, *Jurnal Pendidikan Fisika Indonesia*, **14**, 46 (2018), https://doi.org/10.15294/jpfi.v14i1.9878

[34] H. Zhang, X. Meng, C. Liu, Y. Wang and R. Xiao, *Fuel Process. Technol*., **167**, 484 (2017), https://doi.org/10.1016/j.fuproc.2017.08.007

[35] A. Dave, G. K. Gupta and M. K. Mondal, *Biomass Convers. Biorefin*., **13**, 9289 (2023), https://doi.org/10.1007/s13399-021-01749-7